

Fatigue Strength of Steel Girders Strengthened with Carbon Fiber Reinforced Polymer Patch

M. Tavakkolizadeh, M.ASCE,¹ and H. Saadatmanesh, M.ASCE²

Abstract: Fatigue sensitive details in aging steel girders is one of the common problems that structural engineers are facing today. The design characteristics of steel members can be enhanced significantly by epoxy bonding carbon fiber reinforced polymers (CFRP) laminates to the critically stressed tension areas. This paper presents the results of a study on the retrofitting of notched steel beams with CFRP patches for medium cycle fatigue loading ($R=0.1$). A total of 21 specimens made of S127×4.5 A36 steel beams were prepared and tested. Unretrofitted beams were also tested as control specimens. The steel beams were tested under four point bending with the loading rate of between 5 and 10 Hz. Different constant stress ranges between 69 and 379 MPa were considered. The length and thickness of the patch were kept the same for all the retrofitted specimens. In addition to the number of cycles to failure, changes in the stiffness and crack initiation and growth were monitored during each experiment. The results showed that the CFRP patch not only tends to extend the fatigue life of a detail more than three times, but also decreases the crack growth rate significantly.

DOI: 10.1061/(ASCE)0733-9445(2003)129:2(186)

CE Database keywords: Fiber reinforced polymers; Girders; Crack propagation; Fatigue; Flexure; Retrofitting; Steel.

Introduction

Since 1967, when a mandatory inspection and control on the bridges in the United States were put into place, the American Association of State Highway and Transportation Officials (AASHTO) and the Federal Highway Administration (FHWA) have developed programs to rate bridges through biannual inspection. As a result, it has been found that more than one-third of the highway bridges in the United States are considered substandard. According to the latest National Bridge Inventory (NBI) update, the number of structurally deficient highway bridges in this country is more than 85,000. This does not even include railroad, transient, or pedestrian bridges (FHWA Bridge Program Group 2001).

More than 43% of the bridges in the United States are made of steel. Steel bridges were among the most recommended group for improvement based on the NBI report. The majority of the problems were related to fatigue sensitive details, the need to increase the service load, corrosion, and the lack of proper maintenance (Klaiber et al. 1987). It was also recommended that repair and retrofit be considered before a decision is made to replace a bridge. The cost for rehabilitation and repair in most cases is far less than the cost of replacement. In addition, repair and rehabilitation usually takes less time, reducing service interruption periods. Considering the limited resources available to mitigate the

problems associated with steel bridges, the need for adopting new materials and cost-effective techniques would be evident.

There are more than 120,000 steel highway bridges with welded details in the United States; over 50,000 of them are more than 30 years old. Based on the statistics collected by researchers, generally, major highway bridges experience more than 1.5 million truck passages per year, which can be translated to well over 100 million, or perhaps as high as 300 million, stress cycles in their 100 year lifetime (Moses et al. 1987). Considering the above traffic volume and the age of these bridges, it would be evident that the fatigue limit of 2 million cycles based on design specifications (e.g., AASHTO) underestimates the expected life of bridges.

Before the observation of fatigue cracks in the Yellow Mill Pond Bridge in Bridgeport, Conn., not many steel bridges with cracked details were known (Klaiber et al. 1987). In 11 years after the observation of the first crack in that bridge, cracks in a large number of welded cover plate ends were observed. Fisher studied this problem and concluded that significant fatigue crack growth can occur even after a few high stress cycles (in excess of the fatigue limit), and a large number of accumulating lower stress cycles of over 10 million (Fisher 1997).

CFRP plates or sheets can be epoxy bonded to fatigue sensitive details in steel members to enhance their strength and fatigue life. The superior mechanical and fatigue properties of carbon fiber reinforced plastics (CFRP) make them excellent candidates for repair and retrofit of steel girder bridges. CFRPs are made of high strength carbon filaments (in excess of 2 GPa tensile strength) placed in a resin matrix. They display outstanding mechanical properties with typical tensile strength and modulus of elasticity of more than 1,200 MPa and 140 GPa, respectively. CFRP laminates endure over 1 million cycles of fatigue loading with a stress range of one-half of the ultimate strength (Lorenzo 1986). During the past decade, there have been many studies on repair and retrofit of concrete girders with epoxy bonded fiber reinforced polymer (FRP) materials; however, very few studies

¹Assistant Professor, Dept. of Civil Engineering, Jackson State Univ., Jackson, MS 39217.

²Professor, Dept. of Civil Engineering and Engineering Mechanics, The Univ. of Arizona, Tucson, AZ 85721.

Note. Associate Editor: Mark D. Bowman. Discussion open until July 1, 2003. Separate discussions must be submitted for individual papers. To extend the closing date by one month, a written request must be filed with the ASCE Managing Editor. The manuscript for this paper was submitted for review and possible publication on December 20, 2000; approved on June 11, 2002. This paper is part of the *Journal of Structural Engineering*, Vol. 129, No. 2, February 1, 2003. ©ASCE, ISSN 0733-9445/2003/2-186-196/\$18.00.

have addressed the use of epoxy bonded plates or sheets for strengthening steel girders.

This paper discusses the effectiveness of epoxy bonding CFRP sheets to the fatigue sensitive areas of steel girders to improve their fatigue strength. In this method, the CFRP sheets were used to patch the critical areas of the tension flange in order to reduce the stress level in original elements or carry the stresses across cracked sections.

Previous Work

The use of steel cover plates to repair and strengthen existing structures has been a popular method for rehabilitation of steel girders. The first use of this method can be traced back to 1934 in France, when a bridge constructed in 1861 was strengthened by welding rectangular bars between the rows of rivets (Klaiber et al. 1987). The major shortcomings of welded cover plates are as follows: (1) The need for heavy machinery in order to place the heavy steel plates in place and attaching them; (2) the sensitivity of the welded detail to fatigue; and (3) the possibility of galvanic corrosion between the plate and existing member and attachment materials (weld, bolt, rivet).

Based on the AASHTO Fatigue Specifications (AASHTO 2000), steel girders with welded cover plates fall in the lowest fatigue category, that is category E, at the vicinity of the cover plate termination points. Different geometrical shapes for the cover plate ends or the presence of transverse weld at the cover plate end do not affect the fatigue life of such details (Fisher 1977). A summary of test data on welded plate girders shows that the fatigue life of a cover plated beam is about 45% of a welded plate girder without any attachments (Fisher 1997).

A study of parameters affecting the fatigue strength of cover plated beams leads to the conclusion that the most important parameter is the stress range. Steel grade and stress level do not have much effect on the fatigue life of the member. The reason is the presence of high residual tensile stresses (close to the yield value) due to a nonuniform cooling process after rolling or welding. As a result, regardless of the loading level, or the material yield point, in the neighborhood of transverse welds and corners, the steel will be subjected to full stress cycles.

The possibility of using CFRP in the repair of steel-concrete composite bridges was investigated at the Univ. of South Florida (Sen and Liby 1994). They tested a total of six 6.10 m long beams made of a W203×10.9 steel section attached to a 711 mm wide by a 115 mm thick concrete slab. The CFRP sheets used in the study were 3.65 m long, 150 mm wide, and had two different thicknesses of 2 mm and 5 mm. It was reported that CFRP laminates could considerably improve the ultimate capacity of composite beams.

In another study conducted by the authors at the University of Arizona, effectiveness of the epoxy bonding of the CFRP laminate to intact and damaged steel-concrete composite girders for the strengthening and repair was investigated (Tavakkolizadeh and Saadatmanesh 2003a,b). A total of six composite beams made with a W355×13.6 steel section and a 75 mm thick by 910 mm wide concrete slab were tested. They reported that the CFRP sheets could significantly increase the ultimate load carrying capacity of the intact girders and restore the ultimate load carrying capacity and stiffness of damaged composite girders.

The advantages of using advanced composite materials in the rehabilitation of deteriorating bridges were also investigated at the University of Delaware (Mertz and Gillespie 1996). As a part

of their small-scale tests, they retrofitted eight 1.52 m long W8 × 10 steel beams using five different retrofitting schemes. They reported an average of 60% strength increase in CFRP retrofitted systems. They also tested and repaired two 6.4 m long corroded steel girders. The girders were typical American Standard I shape with depth of 61 cm and flange width of 23 cm. Their results showed an average of 25% increase in stiffness and 100% increase in the ultimate load carrying capacity.

No study on the fatigue behavior of a steel beam retrofitted with epoxy bonded CFRP was found in the literature. However, in a study conducted at the University of Maryland, adhesive bonding and end bolting of steel cover plates to steel girders provided a substantial improvement in the fatigue life of the system (Albrecht et al. 1984). They reported an increase in the fatigue life of more than 20 times compared to the welded cover plates.

In another study, Loher explored the use of this technique in the reinforcement of lightweight aluminum (Loher et al. 1996). They used this method to strengthen and stiffen lightweight aluminum structures and studied the behavior of this system under static and fatigue loading. In their study 0.5 m long specimens, made of an aluminum box with the dimension of 50 mm × 50 mm and a wall thickness of 2 mm, were tested. The CFRP laminates were unidirectional with a fiber content of 66% and an ultimate tensile strength and strain of 2,700 MPa and 1.51%, respectively. These laminates were 50 mm wide and 1 mm thick. They considered two strengthening designs: integral and partial. The integral design was more suitable for strengthening and stiffening while the partial design was suitable for the reinforcement of critical locations for fatigue such as notches and welds. A three-point bending setup was used for static testing and a four-point bending setup for fatigue. Significant improvements in strength (an increase of 115%) were reported only when more than three-quarters of the span was covered by CFRP, while the stiffness was increased linearly when more than one-quarter of the span was covered (80% to 150% increase). For fatigue tests, the beams were cut in the middle and then butt welded together to make a fatigue sensitive detail. The frequency of loading was kept below 30 Hz in order to avoid any misleading results. Adhesives are prone to creep. Therefore, under a high rate of loading, adhesives are not able to undergo creep and their strength increases. Meanwhile, higher frequency tends to generate heat in the adhesive layer and composite sheet, which may result in a change of properties. They reported a significant improvement in the fatigue life of the retrofitted aluminum beams. Their test results showed that retrofitted beams could withstand at least twice the stress range of the unretrofitted beams for the same number of cycles.

Experimental Study

The effectiveness of CFRP sheets on improving fatigue strength of steel girders was examined by testing a number of small-scale steel beams strengthened with pultruded carbon fiber sheets. In order to create a fatigue sensitive detail, tension flanges of steel beams were cut to create a notch on each side. The CFRP patches with identical lengths were then bonded on to the cut sections. Different stress ranges of 69 to 379 MPa were considered in the study.

Materials

Epoxy. A two-component epoxy was used for bonding the laminate to the steel flange surface. The mixing ratio of the epoxy was

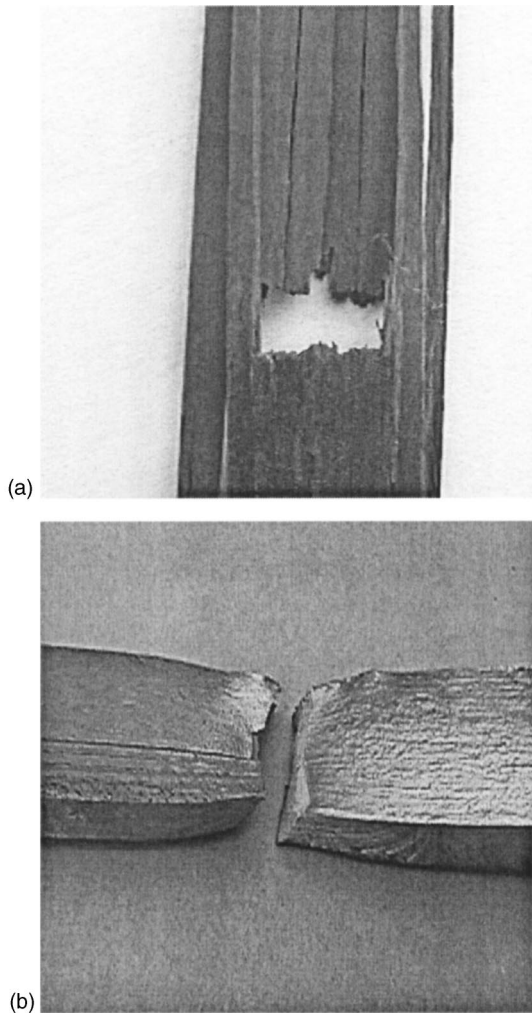


Fig. 1. Typical failed specimens: (a) CFRP coupon and (b) steel coupon

one part resin (bisphenol A based) to one part hardener (polyethylenepolyamin) by volume. The epoxy had a pot life of 30 min at room temperature and was fully cured after 2 days at 25°C.

CFRP. A unidirectional pultruded carbon sheet with a width of 76 mm and a thickness of 1.27 mm was used in the study. After testing a total of 16 straight strips with a length of 400 mm and a width of 25 mm, an average tensile strength of 2,137 MPa, tensile modulus of elasticity of 144.0 GPa, and Poisson's ratio of 0.34 were obtained for the specimens tested. A typical specimen at failure is shown in Fig. 1(a).

Steel. In order to facilitate testing in a universal testing machine, S127×4.5 A36 hot rolled sections were used for the experiments. A total of six dogbone specimens with a gauge length of 100 mm, gauge width of 19 mm, and thickness of 5.4 mm were tested in uniaxial tension. Average yield strengths of 336.4 and 330.9 MPa, modulus of elasticities of 194.4 and 199.9 GPa, and Poisson's ratios of 0.308 and 0.298 were obtained for specimens cut from the flange and web, respectively. A typical specimen at failure is shown in Fig. 1(b).

Specimen Preparation

The steel sections were first cut into 1.3 m long spans. Then, both edges of the tension flange at midspan were cut by a band saw

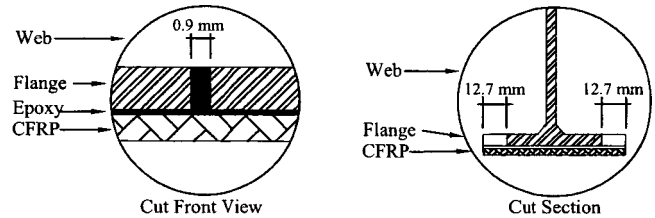


Fig. 2. Schematic of cuts in tension flange

with a blade thickness of 0.9 mm. This created two throughcuts in the tension flange of each specimen. The length of the cuts was controlled with a stopper and kept at 12.7 mm with ± 0.05 mm tolerance as shown in Fig. 2. Each specimen was sand blasted thoroughly by No. 50 glass bids, washed with saline solution, and rinsed with fresh water just before applying the composite sheet in order to avoid oxidation.

CFRP sheets were cut to the length of 300 mm with a band saw. The ends of the sheets were finished smoothly using grid 150 sand paper. After finishing, the sheets were washed with saline solution and rinsed with fresh water.

Upon drying of the steel beam and the CFRP sheet, the epoxy was mixed and applied onto the beam and the sheet. Both pieces were covered with uniform and thin layers of epoxy and were squeezed together to force the extra epoxy and any air pockets to bleed out. Using paper clips, the edges of the CFRP sheet throughout its length were secured while the epoxy was curing. After 2 h, the extra epoxy around the bond area was scraped off and the surface of the sheet was cleaned with acetone. A typical retrofitted specimen is shown in Fig. 3.

After 48 h, two 6 mm long strain gauges with a resistance of 120 ohms were mounted along the edges in the middle of the CFRP sheet below the cuts. For one of the unretrofitted beams two strain gauges were mounted on the tension flange face away from the tip of the cuts.

Experimental Setup

The four-point bending tests were performed using an MTS-810 testing machine. A special bending fixture was constructed to allow the placement of beam specimens in the testing machine. The load was measured by an MTS-661.31E-01 load cell with

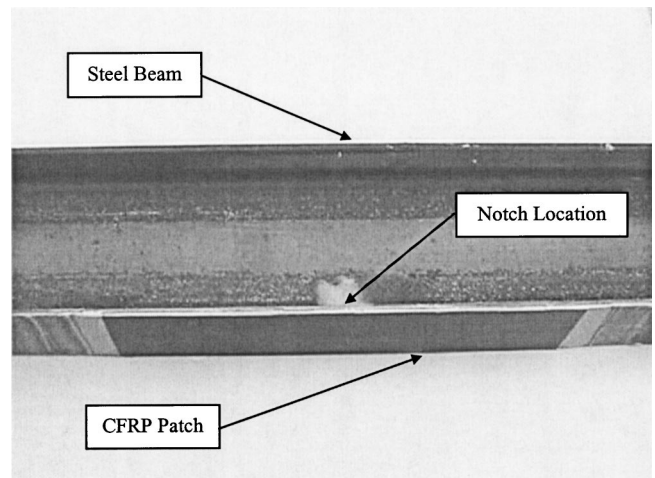


Fig. 3. Typical retrofitted specimens

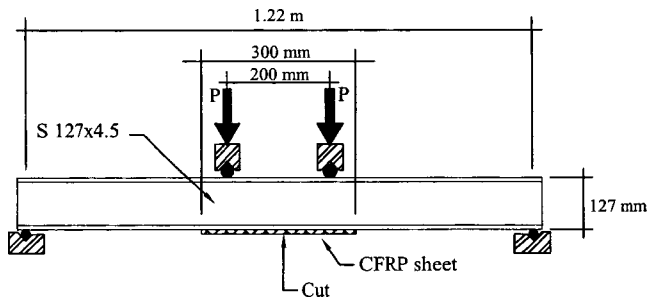


Fig. 4. Schematic of loading setup

capacity of 2,000 kN and the deflection was measured by a DUNCAN 600 series transducer with a range of ± 75 mm. The clear span was 1.22 m and the loading points were 200 mm apart as shown in Fig. 4. In order to prevent any movement of the specimen during the experiments, two ends of the beam were tied down to the roller supports using two steel brackets. The loading blocks were designed with a counter seat for the compression flange to prevent their movement during the experiment. The test setup is shown in Fig. 5.

At first, the unretrofitted beam with strain gauges was tested under displacement control mode with a cross-head movement rate of 0.1 mm/sec. During three loading and unloading cycles, the average strains at the face of the tension flange were monitored. A total of 15 unretrofitted specimens and six retrofitted specimens were tested under different stress range cycles ($R = 0.1$). The cyclic loading was performed under the load control mode for nine different stress ranges. Loading was applied in consecutive half-sine shape segments with a frequency of 5 to 10 Hz. A retrofitting system under this frequency range did not illustrate any noticeable increase in temperature that could affect the bond or properties of the epoxy. A typical cyclic loading was conducted in three separate stages: (1) start to 10,000 cycles, (2) 10,000 to 100,000 cycles (or failure), and (3) 100,000 cycles to failure. The values of load and midspan deflection were recorded

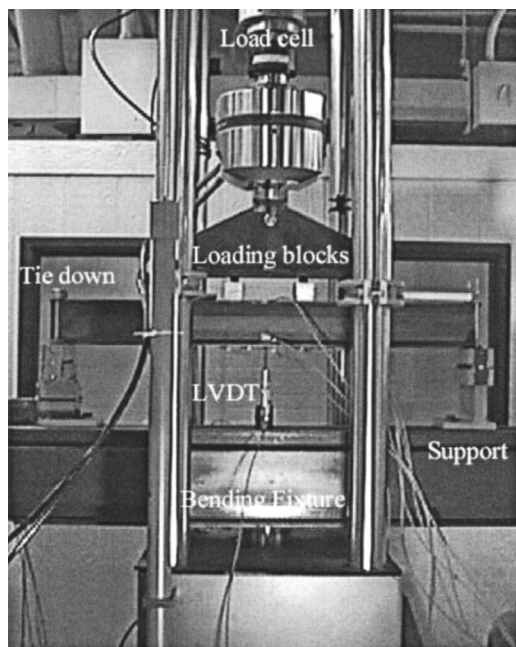


Fig. 5. Test setup

for three complete cycles every 200, 2,000 and 5,000 cycles for first, second, and third stage (if applicable), respectively.

The initiation and growth of cracks were monitored using a magnifying glass and the length of the crack for specified number of cycles was recorded. In order to facilitate the observation, a permanent marker and acetone were used periodically as a penetrating dye. The test stopped when the growth of the crack caused excessive midspan deflection of 5 mm or more compared to the initial elastic deflection.

Evaluation of the Results and Analysis

As was mentioned before, the average stress in the tension flange of an unretrofitted beam was measured using strain gauges mounted on the bottom flange surface at the midspan of one specimen. The average values of six loading and unloading cycles (elastic range) were analyzed. A linear regression analysis was performed and the relationship between average stress and transverse load was established as

$$\sigma = 4,856 P \quad (1)$$

where σ = stress in MPa and P = load in kN. The coefficient of regression for the analysis was 0.998.

AASHTO Design Curves

The current fatigue design curves for redundant structures can be obtained from AASHTO LRFD Bridge Design Specifications (AASHTO 2000). Six major fatigue categories are listed in these specifications, categories A through E, and two subcategories of C' and E' for various details. Fig. 6 displays a plot of stress range versus the number of cycles for AASHTO categories A through E based on all the available fatigue data (Keating and Fisher 1986). For a number of cycles of less than 100,000, extrapolation can be performed and the fatigue design regions for medium cycle fatigue can be established. The data points obtained in this study for unretrofitted and retrofitted specimens are also plotted in Fig. 6. It can be seen that the data points for unretrofitted cut specimens lay between categories C and D while the retrofitted data points lay between categories B and C, as shown in Fig. 6. This was the first positive outcome of the patching technique, which suggested that by applying the patch to a fatigue sensitive detail the fatigue life of the detail could be upgraded for at least one category.

Reliability Based Design Curves

The occurrence of the majority of natural phenomenon follows the normal distribution with two parameters of mean and standard deviation, which are random variables. The mean value cannot be used directly in the design. In order to establish design values for engineering applications, a conservative value, which is smaller than the mean value, is usually considered. The difference between the design value and the mean value depends on the variation of the data, the number of data points, the desired confidence, and the desired probability of survival. The design value can be expressed according to the following relationship:

$$X_D = X_M - K_{p,\gamma,n} S_X \quad (2)$$

where X_D = design value; X_M = mean value; S_X = standard deviation, p = probability of survival in percent; γ = confidence level in percent; n = number of data points; and $K_{p,\gamma,n}$ = one-sided tolerance limit factor. $K_{p,\gamma,n}$ is proportional to the values of p and γ

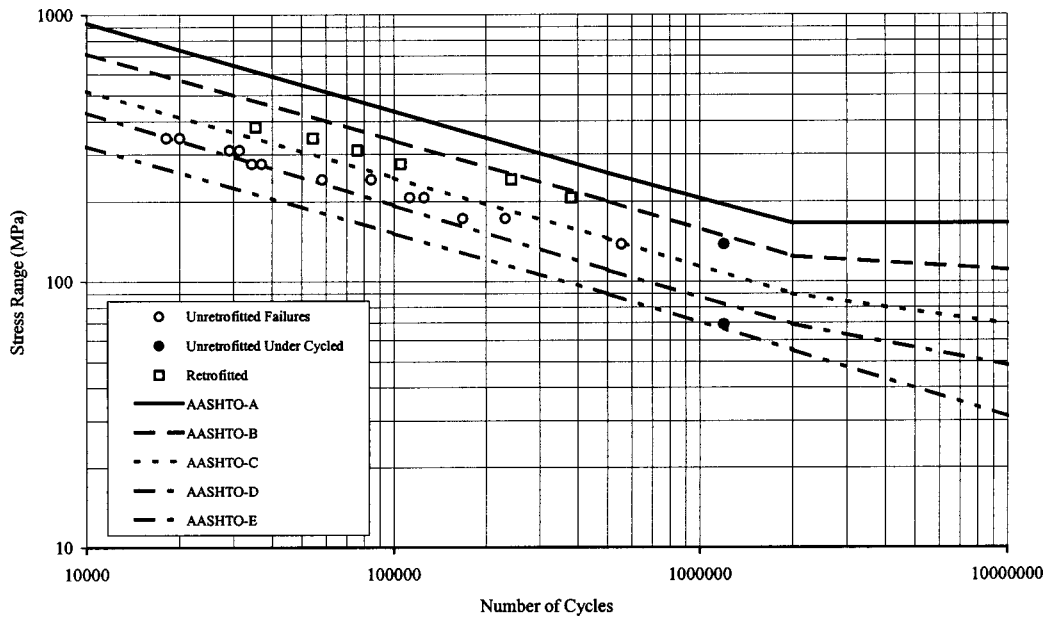


Fig. 6. *S-N* plot for all data points and AASHTO categories

and inversely proportional to the value of n . The values of tolerance limit factors can be obtained from different statistical references (Naterella 1963). Using this method, the “design value” is determined as the “value,” where a certain percentage (p) of the population will lay above that value. The confidence associated with the previous prediction is represented with γ .

In the fatigue case, establishment of the design *S-N* line is the objective, but the concept would be fairly similar. A linear *S-N* relationship in log-log space for fatigue data is a very common assumption and the following equations are usually used:

$$NS^m = A \quad (3)$$

$$\log S = 1/m \log A - 1/m \log N \quad (4)$$

where N = number of cycles to failure; S = stress range; m = inverse of the slope; and A = fatigue constant. The least square analysis can be performed in order to obtain these parameters.

A common approach in establishing the design *S-N* line is to consider a line parallel to the least square line, but shifted to the left (safe side) by a certain amount. In other words, only the intercept of the line is assumed to be a random variable and the slope of the line is considered to be a constant. The amount of shifting depends on the variation of the data, the number of data points, the desired confidence level, and the desired probability of survival. The design line is expressed as

$$NS^m = A_0 \quad (5)$$

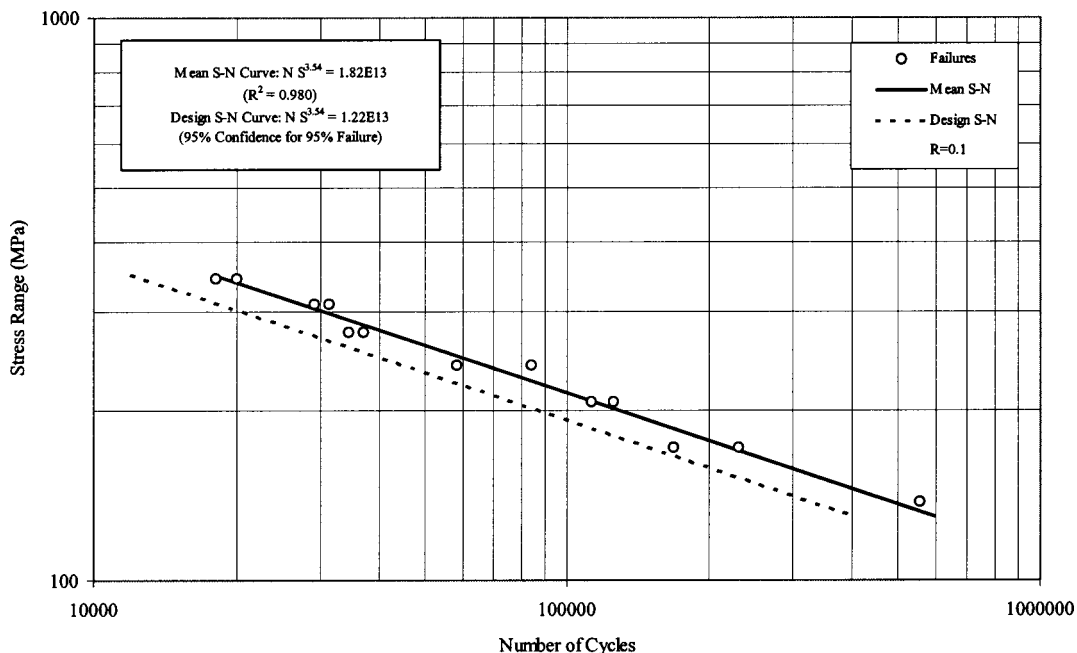


Fig. 7. *S-N* plot and design curve for unretrofitted samples

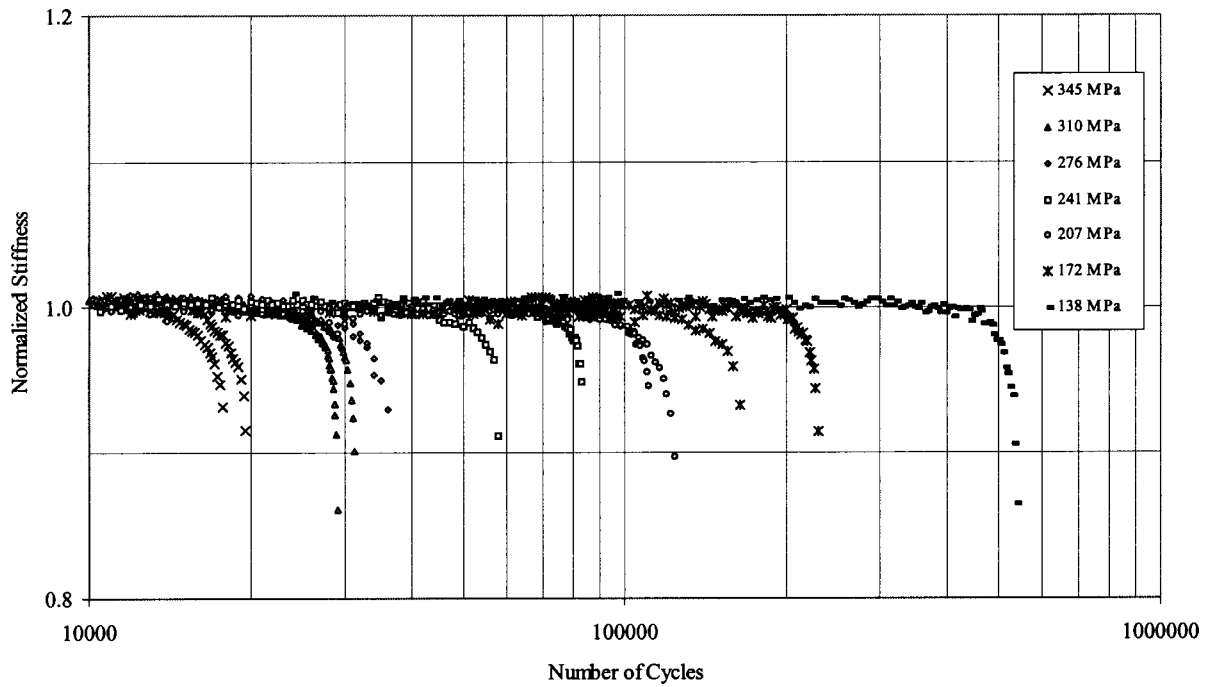


Fig. 8. Change in stiffness of unretrofitted beams during fatigue tests

$$\log A_0 = \log A - K_{p,\gamma,n} S_R \quad (6)$$

$$S_R^2 = 1/(n-2) \sum (y_i - y_i^{LSL})^2 \quad (7)$$

where A_0 = design fatigue constant; S_R = least square deviation; y_i = actual value (fatigue life); and y_i^{LSL} = estimated value (fatigue life) by least square line. As can be seen, instead of considering the standard deviation, S_X , which represents the deviation of the data points from the mean value, a different statistical parameter, S_R , which represents the deviation of the data points from the least square line is considered.

Using the techniques described here for establishing design curves, the tolerance interval with 95% confidence level for 95% survival was used similar to those used in the AASHTO specifications (Fisher 1997). The values of $K_{95\%,95\%,.6}$ and $K_{95\%,95\%,.13}$ for a one-sided tolerance limit for normal distribution are 3.707 and 2.670, respectively (Natrella 1963).

Unretrofitted Beams

In order to establish a reliable set of control data, seven pairs of unretrofitted beams were subjected to constant stress range cycles of 138, 172, 207, 241, 276, 310 and 345 MPa. One unretrofitted beam was subjected to the stress range of 69 MPa also. Among all of the unretrofitted specimens, only two specimens at stress ranges of 69 and 138 MPa did not fail before 1,200,000 cycles as shown in Fig. 6 with solid circles (under cycled).

Fatigue life. The test results of all unretrofitted specimens that were failed during the experiments are shown in Fig. 7. The relationship between the number of cycles to failure and the stress range in a log-log space was linear. Therefore, a linear regression of the data points, not containing the run-out, resulted in the mean $S-N$ line with a coefficient of regression of 0.980. Using reliability techniques discussed earlier, 95% confidence level for 95% sur-

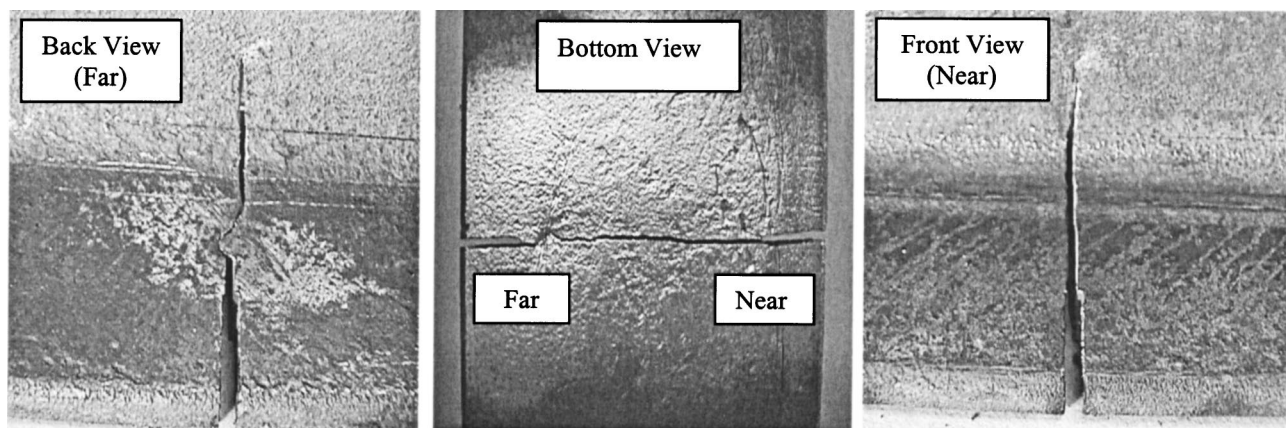


Fig. 9. Typical failure of an unretrofitted beam

Table 1. Number of Cycles for Crack Initiation and Failure (Unretrofitted Beams)

Stress range (MPa)	Number of Cycles	
	Crack Initiation	Failure
207	69,760	119,140
241	32,495	71,278
276	14,511	35,710
310	10,019	30,216
345	7,606	19,068

vival was used for establishing the design line. Both lines are also plotted in Fig. 7, and their respective equations are as follows:

$$\text{Mean } S-N \text{ curve: } \log S = 13.260 - 0.282 \log N \quad (8)$$

$$\text{Design } S-N \text{ curve: } \log S = 13.086 - 0.282 \log N \quad (9)$$

The slopes of the lines ($1/[-3.54] = -0.282$) were less steep as compared to the AASHTO curves categories C and D with the slopes of -0.308 and -0.326 , respectively. The smaller slope suggested longer fatigue life especially under high cycle fatigue. This could be due to the size of the specimens tested in this study. Researchers have shown that the results of small-scale testing overestimate the fatigue strength of beams (Fisher 1977).

Stiffness changes. Throughout the majority of fatigue experiments, the stiffness (ratio of load to midspan deflection) of the beam remained constant. When the crack grew longer than 10 mm, and before reaching the fillet, the stiffness of the beam started to decrease and in a short period the beam failed. The normalized values of the stiffness for each failed, unretrofitted specimen versus number of cycles are shown in Fig. 8. By looking at the failure points, it can be seen that unretrofitted beams failed before their stiffness dropped by more than 10%.

Crack initiation and propagation. The crack initiation and

propagation in all unretrofitted specimens were similar. In order to simplify describing the crack growth record, the terms “near” and “far” were used that corresponded to the side that the crack initiated and the side that the crack terminated, respectively. The crack always initiated from the tip of one of the cuts. Then, the crack started to move toward the near web/flange junction. After reaching the top of the near fillet section of the web, it continued to go up on the near side of the web while the crack front was still growing horizontally to reach the far side of the web. In a few remaining cycles of the beam, the crack grew to reach the tip of the opposite cut. The shear failure occurred at the last moment in the far cut tip and caused complete failure of the flange and further rupture of the web until the deflection limit was violated and the experiment was stopped. A typical failed specimen is shown in Fig. 9.

The number of cycles for the crack to become visible (6.4 mm) and to reach the near fillet (16.5 mm), near web (23 mm), far web (28 mm), and far cut tip (51 mm) were recorded and their average values for different stress ranges were calculated. By considering the first two crack lengths (6.4 and 16.5 mm) and their corresponding number of cycles, and performing a linear extrapolation, the number of cycles for the crack initiation can be estimated. These values are presented in Table 1. Fig. 10 displays a plot of the crack length versus the number of cycles after crack initiation.

For a crack length of less than 20 mm, the specimens exhibited a stable crack growth (constant crack growth rate) under various stress ranges. The stable crack growth rates were established by linear interpolation of the data points. The rates of 0.52, 0.62, 1.15, 1.23, and 2.09 $\mu\text{m}/\text{cycle}$ for the stress ranges of 207, 241, 276, 310, and 345 MPa were obtained. The number of cycles and the crack length in which stiffness decay was apparent are displayed with solid circles (stiffness drops) in Fig. 10. The decrease in the stiffness in all of the specimens was detected when the crack length was between 13 and 15 mm.

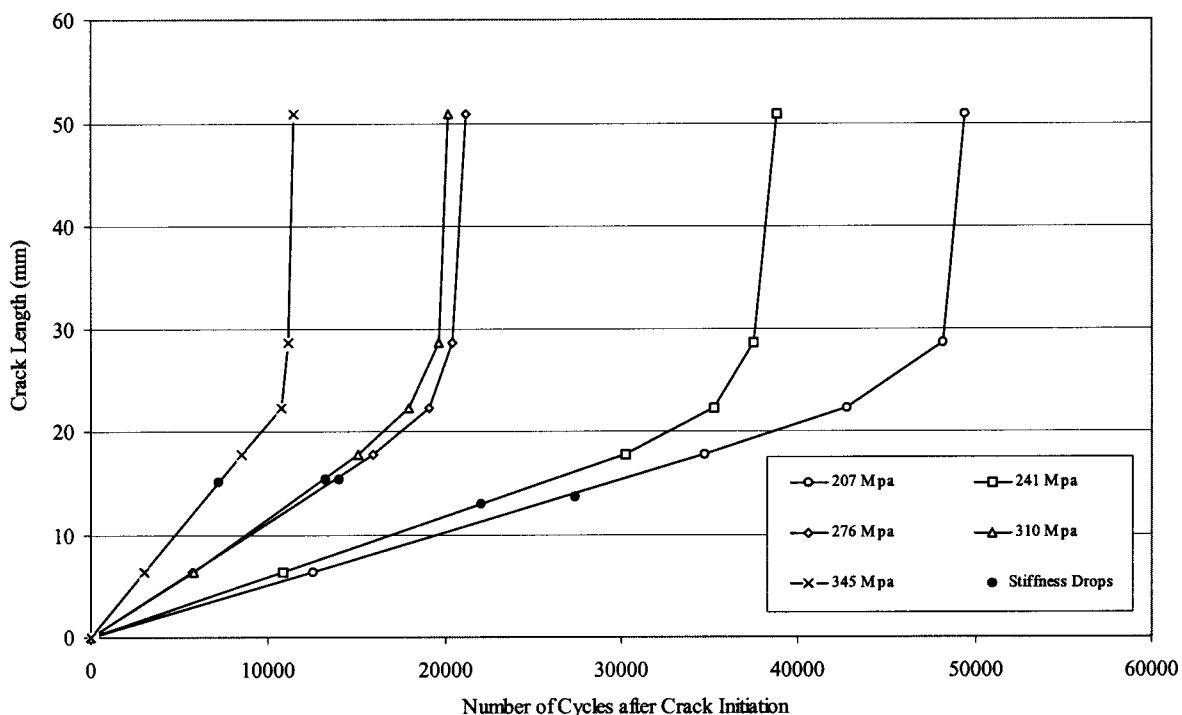


Fig. 10. Change in crack length for unretrofitted beams during fatigue tests

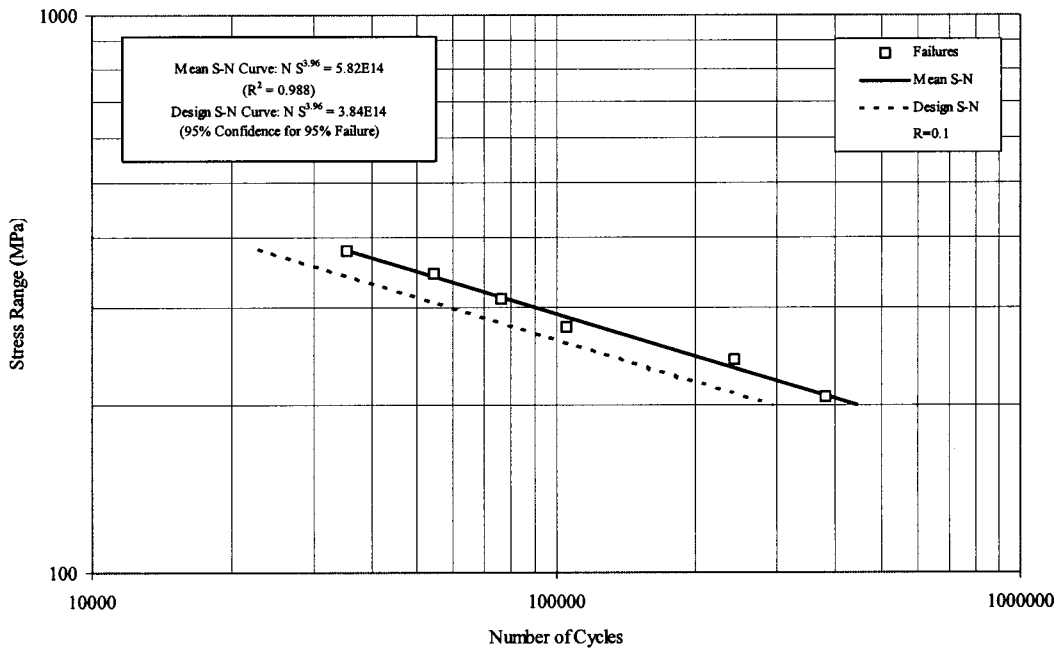


Fig. 11. *S-N* plot and design curve for retrofitted beams

Retrofitted Beams

After close consideration of the test results of unretrofitted specimens, it was decided to conduct the fatigue test of retrofitted beams under higher stress ranges. The three lower stress ranges were eliminated, and the stress range of 379 MPa was added. Therefore, a total of six retrofitted beams were subjected to constant stress range cycles of 207, 241, 276, 310, 345, and 379 MPa. As a result, there was not any undercycled specimen in this group. The data points were plotted and are shown in Fig. 11.

Fatigue life. Similar to unretrofitted beams, the number of cycles to failure and the stress range had a linear log-log relationship. Therefore, a linear regression of the data points resulted in the mean *S-N* line with a coefficient of regression of 0.988. Using the same reliability techniques mentioned before, the design curve for retrofitted beams was established. Both lines are plotted in Fig. 11, and their respective equations are as follows:

$$\text{Mean } S-N \text{ curve: } \log S = 14.765 - 0.253 \log N \quad (10)$$

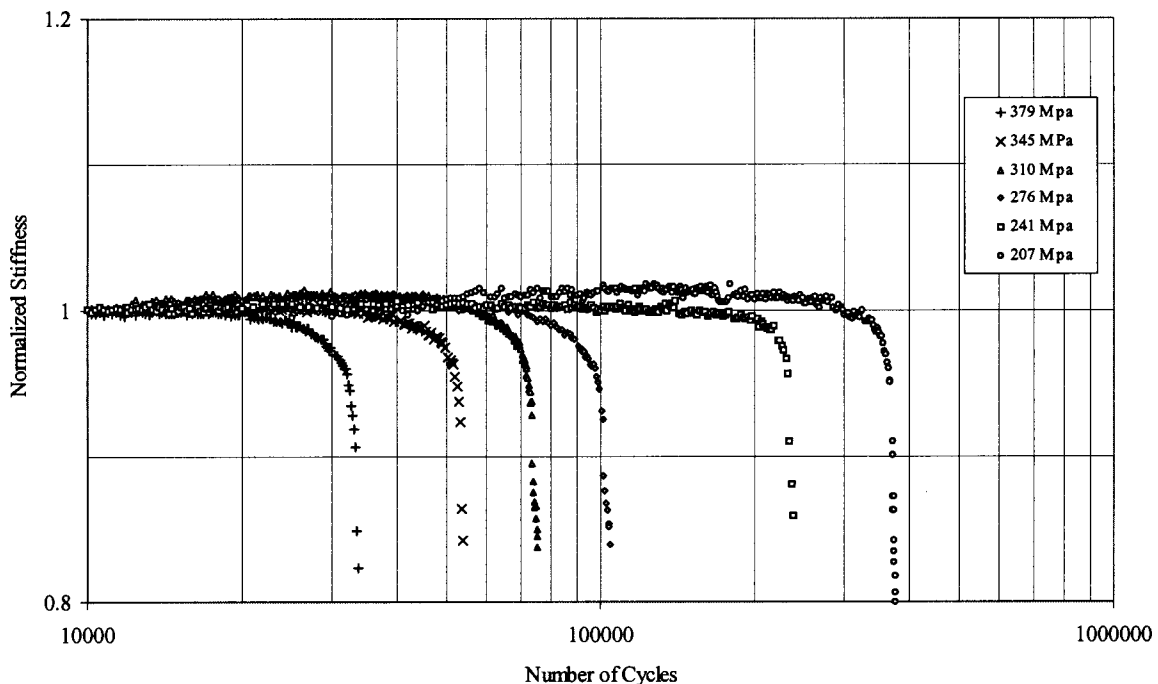


Fig. 12. Change in stiffness of retrofitted beams during fatigue tests

Table 2. Number of Cycles for Crack Initiation and Failure (Retrofitted Beams)

Stress range (MPa)	Number of Cycles	
	Crack Initiation	Failure
207	152,414	379,824
241	92,687	241,965
276	35,966	105,345
310	21,655	75,910
345	16,786	54,300
379	7,146	35,356

$$\text{Design } S-N \text{ curve: } \log S = 14.584 - 0.253 \log N \quad (11)$$

The slope of these lines ($1/[-3.96] = -0.253$) was smaller than the slope of the unretrofitted lines (-0.282) and the lines were also less steep as compared to the AASHTO curves in categories B and C with the slopes of -0.297 and -0.308 , respectively. The smaller slope was an indication of longer fatigue life especially under high cycle fatigue. This could be due to the size of the specimens tested in this study.

Stiffness changes. Considering the small length and thickness of the CFRP patch, the initial elastic stiffnesses of retrofitted and unretrofitted beams were similar. During the best part of fatigue cycling, the stiffness of the beam remained constant and was similar to the unretrofitted beams. Only after the visible crack started to grow in the flange and passed the fillet did the stiffness of the beam start to decrease, and in a short time after that the beam failed. The normalized values of stiffness for each failed retrofitted specimens versus the number of cycles were plotted and are shown in Fig. 12. By looking at the failure points, it can be seen that the retrofitted beams failed when their stiffness dropped by approximately 17%, a notable difference compared to the unretrofitted beams that failed before a 10% drop in stiffness. Stiffness drop and an increase in deformation can act as an advanced warning before failure and prevent additional property losses.

Crack initiation and propagation. The crack initiation and propagation in all retrofitted beams were similar, but different from those of unretrofitted specimens. Table 2 shows the number of cycles required for a fatigue crack to start under different stress ranges. The crack always initiated from the tip of one of the cuts. The crack then started to move toward the web. The terms “near” and “far” were used to identify the side that crack initiated and

the side that the crack terminated, respectively. After reaching the fillet section of the web, debonding at the near edge of the CFRP sheet started. While the crack front moved to the far side, the debonding at the edge continued to grow. Even after the crack front reached the far cut tip, the debonding remained fairly stable (constant rate of debonding). At this stage, the far edge of the CFRP sheet started to debond. Except for the 207 MPa stress range, the failure of the sheet happened after approximately 50 mm of debonding on each side of the notch on both edges. A typical failed specimen is shown in Fig. 13.

During the experiments, for monitoring the crack growth, the same crack lengths as those for unretrofitted specimens were considered and the number of cycles for reaching those specified lengths were recorded for different stress ranges. Linear extrapolations similar to the previous section resulted in an estimate of the number of cycles for the crack initiation. Fig. 14 displays the relationship between the crack length and the number of cycles after crack initiation.

The stable crack growth rates were established by linear interpolation of data points in the initial stage where crack growth rate is constant. These rates were 0.12, 0.20, 0.41, 0.50, 0.72, and 0.89 $\mu\text{m}/\text{cycle}$ for the stress ranges of 207, 241, 276, 310, 345, and 379 MPa, respectively. These growth rates were between 25% to 40% of the growth rate for unretrofitted beams. After comparing the result of retrofitted beams to those for unretrofitted beams, the benefits of patching in limiting the crack growth were observed. The number of cycles between crack initiation and a complete loss of tension flange increased by factors of 4.5, 3.6, 3.1, 2.5, and 3.2 for the stress ranges of 207, 241, 276, 310, and 345 MPa, respectively.

Similar to unretrofitted specimens, for crack lengths less than 20 mm, the specimens exhibited a stable crack growth under various stress ranges. Solid circles shown in Fig. 14 are representing the beginning of apparent stiffness drop. The decrease in the stiffness for four higher stress ranges began when the crack length was between 19 to 21 mm (the crack front was between near fillet and near web). For the two lower stress ranges, only after the crack lengths reached 25 to 27 mm (the crack front started to grow up in the near web), the stiffness of the beam started to decrease. The numbers of cycles to which the specimens failed are shown in Fig. 14 by solid triangles. The numbers next to the solid triangles indicate additional cycles after the complete loss of the tension flange. The effect of patches in extending the fatigue

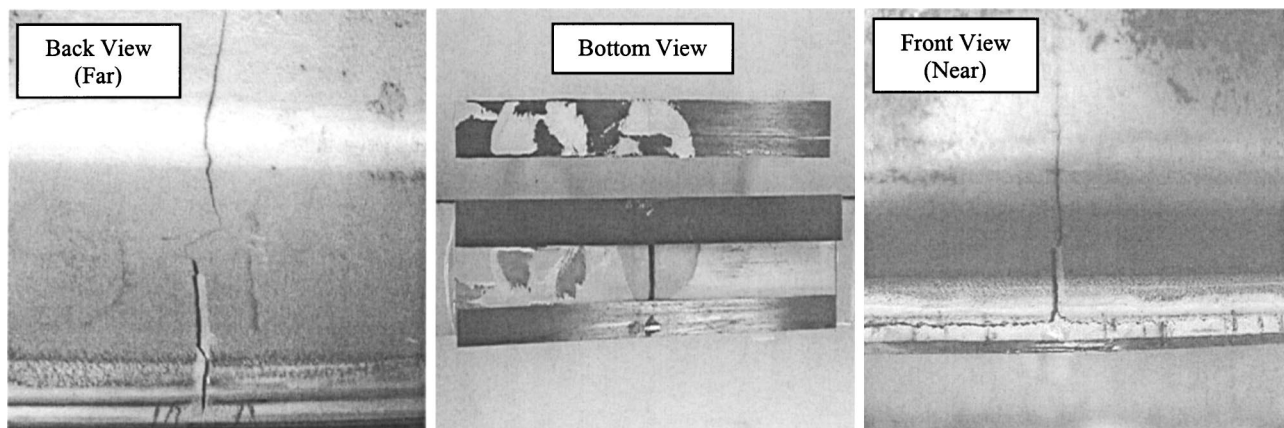


Fig. 13. Typical failure of a retrofitted beam

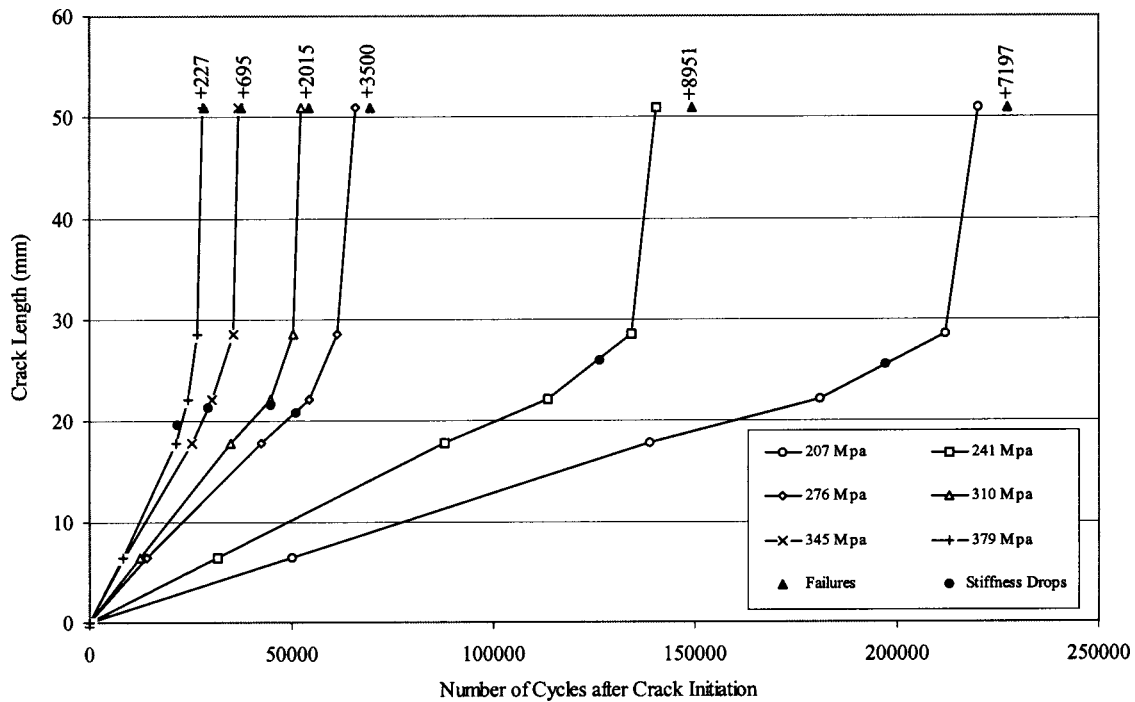


Fig. 14. Change in crack length for retrofitted beams during fatigue tests

life of the beams beyond the total tension flange loss was more pronounced in the lower stress ranges.

Conclusions

Test results from steel beams retrofitted with epoxy bonded CFRP laminates to increase fatigue life are very promising. For all stress ranges considered in this study, this technique improved the fatigue life of the detail significantly. The effect of the CFRP patch on the crack arrest was also notable. Based on the results of the experimental investigation, the following conclusions are drawn:

1. Fatigue life of a detail can be improved by epoxy bonding a CFRP patch to the member. Retrofitted specimens experienced longer fatigue lives of between 2.6 to 3.4 times the unretrofitted specimens for stress ranges of 345 to 207 MPa, respectively. This improvement is equivalent to upgrading the detail from the AASHTO category D to category C.
2. Design $S-N$ curve for unretrofitted and retrofitted cut specimens were $S \cdot N^{3.54} = 1.22 \times 10^{13}$ and $S \cdot N^{3.96} = 3.84 \times 10^{14}$, respectively. The slope of the $S-N$ curves for the specimens (retrofitted and unretrofitted) in a log-log space is slightly smaller than the slope of the AASHTO design curves.
3. The decrease in the stiffness for the unretrofitted specimens occurred at much shorter crack lengths. The unretrofitted specimens showed stiffness decrease, for crack lengths of about 14.5 mm, while retrofitted specimens showed a decrease in stiffness when the cracks grew to about 22.5 mm.
4. In both retrofitted and unretrofitted cases, the crack growth was stable for the crack lengths of up to 20 mm. The stable crack growth rates decreased by an average of 65% as a result of retrofitting.
5. The average total number of cycles to failure after crack initiation for retrofitted specimens was 3.5 times the one for unretrofitted specimens. The retrofitted specimens were able

to carry a few extra cycles even after the tension flange had completely cracked, especially under lower stress ranges.

6. Since the medium cycle fatigue in this study was investigated (less than 1 million cycles) the effect of this retrofitting technique in high cycle fatigue (over 10 million cycles) needs to be further investigated. The long-term durability of the bond and the possibility of galvanic corrosion are issues that also require further investigation. Preliminary work in this area is reported by the authors (Tavakkolizadeh and Saadatmanesh 2001).

Acknowledgments

The writers wish to acknowledge the funding of this research by the National Science Foundation, Grant No. CMS-9413857, Dr. John B. Scalzi, Program Director. The results and conclusions presented here are those of the writers and do not represent the views of the National Science Foundation.

Notation

The following symbols are used in this paper:

- A = fatigue constant;
- A_0 = design fatigue constant;
- $K_{p,\gamma,n}$ = one-sided tolerance limit factor;
- m = inverse of the slope ($S-N$ line);
- N = number of cycles to failure;
- n = number of data points;
- P = load in kN;
- p = survival probability in %;
- S = stress range in MPa;
- S_R = lest square deviation;
- S_X = standard deviation;

X_D = design value;
 X_M = mean value;
 y_i = actual value (fatigue life);
 y_i^{LSL} = estimated value (fatigue life) by least square line;
 γ = confidence level in %; and
 σ = normal stress in MPa.

References

- Albrecht, P., Sahli, A., Crute, D., Albrecht, Ph., and Evans, B. (1984). "Application of adhesive to steel bridges." *Rep. No. FHWA-RD-84-037*, The Federal Highway Administration, Washington, D.C., 106–147.
- American Association of State Highway and Transportation Officials (AASHTO). (2000). *Standard Specifications for Highway Bridges*, 16th Ed., Washington, D.C.
- Federal Highway Administration (FHWA) Bridge Program Group. (2001). "Count of deficient bridges by state non federal-aid highway." (<http://www.fhwa.dot.gov/bridges/britab.htm>) (March 20, 2002). The Office of Bridge Technology, Washington, D.C.
- Fisher, J. W. (1977). "Bridge fatigue guide: Design and details." *Publication T112-11/77*, AISC, New York.
- Fisher, J. W. (1997). "Evaluation of fatigue resistant steel bridges." *Rep. No. TR 1594*, Transportation Research Board, National Academy Press, Washington, D.C.
- Keating, P. B., and Fisher, J. W. (1986). "Evaluation of fatigue tests and design criteria on welded details." *Rep. No. NCHRP 286*, Transportation Research Board, Washington, D.C.
- Klaiber, F. W., Dunker, K. F., Wipf, T. J., and Sanders, W. W. (1987). "Methods of strengthening existing highway bridges." *Rep. No. NCHRP 293*, Transportation Research Board, Washington, D.C.
- Loher, U., Mueller, B., Leutwiler, R., and Esslinger, V. (1996). *CFRP-strengthened aluminum structures*, EMPA Dubendorf, Uberlandstrasse, Dubendorf, Switzerland.
- Lorenzo, L., and Hahn, H. T. (1986). "Fatigue Failure Mechanisms in Unidirectional Composites." *Composite Materials: Fatigue and Fracture*, American Society for Testing and Materials, Philadelphia, 210–232.
- Mertz, D., and Gillespie, J. (1996). "Rehabilitation of steel bridge girders through the application of advanced composite material." *Rep. No. NCHRP 931-ID11*, Transportation Research Board, Washington, D.C., 1–20.
- Moses, F., Schilling, C. G., and Raju, K. S. (1987). "Fatigue evaluation procedures for steel bridges." *NCHRP Rep. No. 299*, Transportation Research Board, Washington, D.C.
- Natrella, M. G. (1963). "Experimental statistics." *National Bureau of Standards Handbook 91*, U.S. Government Printing Office, Washington, D.C.
- Sen, R., and Liby, L. (1994). "Repair of steel composite bridge sections using carbon fiber reinforced plastic laminates." *Rep. No. FDOT-510616*, Florida Department of Transportation, Tallahassee, Fla.
- Tavakkolizadeh, M., and Saadatmanesh, H. (2001). "Galvanic corrosion of carbon and steel in aggressive environments." *J. Compos. Constr.*, 5(3), 200–210.
- Tavakkolizadeh, M., and Saadatmanesh, H. (2003a). "Repair of damaged steel-concrete composite girders using CFRP sheets." *J. Compos. Constr.*, in press.
- Tavakkolizadeh, M., and Saadatmanesh, H. (2003b). "Strengthening of steel-concrete composite girders using carbon fiber reinforced polymers sheets." *J. Struct. Eng.*, 129(1), 30–40.